

Spin exchange in the excitation of spin-polarized Na atoms by Ne^+ -ion impact

W. Jitschin,* S. Osimitsch, H. Reihl, D. W. Mueller,[†] H. Kleinpoppen,[‡] and H. O. Lutz
Fakultät für Physik, Universität Bielefeld, 4800 Bielefeld, Federal Republic of Germany

(Received 24 February 1986)

The $3s$ - $3p$ excitation of spin-polarized Na atoms by Ne^+ ions has been studied for impact energies $E_{\text{lab}}=200$ eV to 6 keV, i.e., in the adiabatic regime. The total excitation cross section and the three Stokes polarization parameters of the fluorescence light have been measured. The linear polarization of the light shows a preferential excitation of the $|m_l|=1$ magnetic substates. The circular polarization probes the spin orientation of the excited $3p$ state. At the highest impact energies investigated the experimental data are compatible with conservation of spin orientation during the collision. With decreasing impact energy, the spin polarization of the final $3p$ state becomes smaller than the spin polarization of the initial $3s$ state. This apparent spin depolarization is attributed to the exchange interaction between the Na valence electron and the unfilled $\text{Ne}^+ 2p^5$ core in the quasimolecule formed during the collision.

I. INTRODUCTION

Atomic-collision processes have been studied for several decades and experiments of increasing degree of sophistication have been performed. According to the historical development various generations of experiments may be distinguished:¹ First-generation experiments measure angle-integrated cross sections, second-generation experiments employ a cylindrically symmetric collision geometry, and in third-generation experiments the symmetry is reduced to planar symmetry. The driving force behind the high sophistication of modern experiments is the prospect of an *ab initio* understanding of the collision process, as well as the development of intuitive concepts for the description of essential features (see, e.g., Ref. 2). Such experiments are characterized by the attempt to extract the maximum information on the collision process, ideally requiring the preparation of "pure" initial eigenstates and a complete analysis of the final states including the spin properties. Corresponding experiments are called "ideal,"³ "perfect,"⁴ or "complete."⁵ These experiments are now state of the art in the field of electron impact and photoionization (see, e.g., Refs. 6 and 7).

In the field of energetic atomic collisions, however, the spin is generally assumed to retain its orientation during the collision and thus to bear no additional information on the collision process (see, e.g., Ref. 1). This assumption seems to be justified regarding the comparatively weak interaction of the spin and its environment via the magnetic moment associated with the spin. If any coupling between spin momenta and orbital angular momenta during the collision is negligible then the total spin, i.e., the vectorial sum of the spins of the two atoms, is conserved; this behavior is known as Wigner's rule.⁸ For excitation processes, the assumption of spin decoupling during the collision but subsequent fine (and hyperfine) coupling (Percival and Seaton hypothesis⁹) has been very successful. Nevertheless, a nonstatistical population of multiplet levels has been observed for ion-atom collisions¹⁰

which shows a breakdown of this hypothesis. Recent advanced experiments clearly indicate that the spin orientation of a target electron may be affected in an ion-atom collision.^{11,12} Spin-affecting mechanisms are the spin-orbit interaction and, in the case of at least two electrons, the electron-exchange interaction (Table I).

In ion-atom collisions, the interaction between the orbital motion and the spin of the projectile is tiny due to the small magnetic field created by the slow motion of an ionic projectile (in contrast to electron impact^{13,14}). Thus the projectile's trajectory is hardly influenced by its spin orientation. On the other hand, spin-orbit coupling of individual electrons of the target atom (and the projectile) may cause a precession of their spin orientation in space. Due to the weakness of the spin-orbit interaction this precession is comparatively slow and it is very reasonable to

TABLE I. Spin-affecting interactions in collisions of an impinging (quasi) one-electron atom or an electron with a one-electron target atom.

Type of interaction	Projectile	
	One-electron atom	Electron
spin-orbit interaction between	orbit and spin of the electron at the projectile	
	orbit of projectile and projectile spin	orbit and spin of impinging electron
	orbit and spin of the electron at the target atom	orbit and spin of the electron at the target atom
exchange of	electron at the projectile and electron at the target atom	incoming electron and electron at the target atom

assume an almost space-fixed (“frozen”) spin orientation during some region of the collision.¹⁵ However, if the orbital angular momentum of an electron is affected in the collision, spin-orbit interaction at larger internuclear separations may entail an apparent change of its spin orientation. Detailed quantum-mechanical treatments of the dynamics of this spin-coupling process are available (see, e.g., Refs. 16 and 17). In the case of at least two active electrons the spin orientation of an individual electron may also be affected by the interchange of electrons. According to Pauli’s principle (antisymmetric total wave function), the spin properties are coupled to spatial symmetry properties. As the electrostatic electron-electron repulsion is strong, electron exchange may strongly change the spin orientation. This has been shown experimentally for thermal collisions^{18,19} and has been predicted theoretically for energetic collisions.^{20,21} Both spin-affecting mechanisms exhibit different symmetry properties²² which allows an experimental separation of the mechanisms as has been demonstrated for electron-atom collisions.²³

As a first step towards experiments in energetic atomic collisions in which the spin behavior is explicitly studied and which finally will give truly complete information on the collision process,²⁴ we have investigated the ion-impact $3s\text{-}3p$ excitation of spin-polarized Na atoms. The collision-induced spin change has been determined by a polarization analysis of the fluorescence light emitted in the decay of the $3p$ state.

II. EXPERIMENTAL PROCEDURE

The experimental setup is sketched in Fig. 1; it consists basically of a crossed-beam apparatus. The Na atoms are produced in a two-stage oven; by heating the nozzle chamber to temperatures higher than the oven chamber the dimer content in the beam is strongly reduced.^{25,26} The Na beam is spin polarized by a hexapole magnet. A guiding magnetic field of approximately 10^{-4} T defines the quantization axis of the spin polarization P and fixes the direction of spin orientation after the hexapole. The Na beam is intersected by an Ne^+ -ion beam at a right angle. The ions are delivered from a commercial ion source (Colutron); a mass-analyzer with crossed electric and magnetic fields (Wien filter) selects $^{20}\text{Ne}^+$ ions and suppresses $^{22}\text{Ne}^+$ ions and contaminations of the ion beam. The ion source can also be used as an electron source by reversing the acceleration and focusing voltages. The ion or electron beam is focused into the interaction region and collected in a three-stage Faraday cup. By

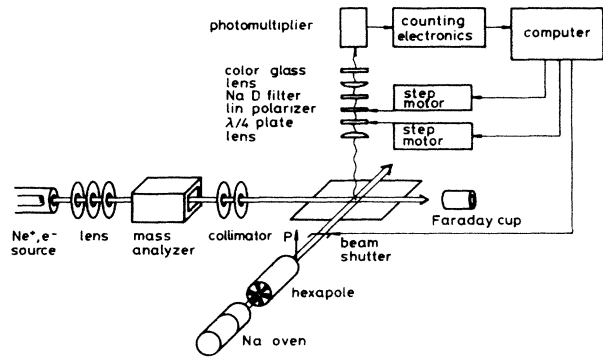


FIG. 1. Sketch of the experimental setup.

sooting the walls^{27,28} and placing a cone at the bottom of the Faraday cup²⁹ the emission of secondary electrons is minimized. The collision-induced excitation of the Na $3p$ state is detected via the emitted resonance fluorescence.

The collision geometry deserves special attention. An arrangement with transverse spin polarization is advantageous in a noncoincident experiment. All relevant information on the excited state can be obtained from the polarization properties of the fluorescence light emitted in the direction of spin orientation.³⁰ This scattering arrangement is analogous to the use of transversely polarized electrons in polarized-electron–unpolarized-atom experiments.²³ The polarization analysis of the light is performed by a $\lambda/4$ retardation plate and a linear polarizer. Light from the unresolved Na $D_{1,2}$ doublet line is selected by an interference filter (Spindler and Hoyer 371108) and a color filter (Spindler and Hoyer OG 530) and detected by a photomultiplier with a bialkali cathode (EMI 9789B). Data accumulation is controlled by a computer: photons are counted during a preselected time interval for different angular settings of retardation plate and linear polarizer as well as for the Na beam switched on and off. The light signal obtained with the Na beam (shutter open) typically is larger by one order of magnitude than the signal without the Na beam (shutter closed). The light polarization is analyzed in terms of the Stokes polarization parameters P_1 , P_2 , and P_3 ³¹ by rotating the optical components. P_1 denotes the linear polarization with respect to an axis parallel to the impact direction, P_2 the linear polarization with respect to an axis tilted by 45° to the impact direction, and P_3 the circular polarization. Depending on the angular settings of the retardation plate and the linear polarizer the relative transmission T of the optical system is given by

$$2T(\beta, \alpha - \beta) = 1 + P_1 \{ \cos(2\beta) \cos[2(\alpha - \beta)] - \sin(2\beta) \sin[2(\alpha - \beta)] \cos \Delta \} \\ + P_2 \{ \sin(2\beta) \cos[2(\alpha - \beta)] + \cos(2\beta) \sin[2(\alpha - \beta)] \cos \Delta \} + P_3 \{ \sin[2(\alpha - \beta)] \sin \Delta \}, \quad (1)$$

where α and β denote the rotation angles of the retardation plate and the linear polarizer with respect to the impact axis (Fig. 2). Δ is the phase retardation of the retardation plate. The optical system was carefully checked. For example, a slight offset of the linear polarizer setting

from the impact direction would transform some part of the P_1 polarization into P_2 . The linear polarizer consisting of a dichroitic polymer film has a measured extinction ratio better than 10^{-3} and may be regarded as ideal. In contrast, the retardation of the retardation plate was

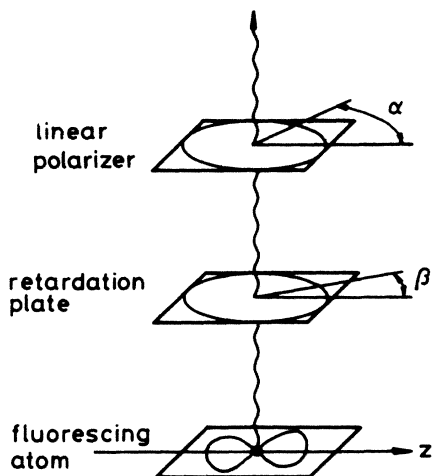


FIG. 2. Arrangement of optical components for measuring the Stokes polarization parameters of the fluorescence light.

found to deviate from the nominal value $\Delta=90^\circ$ by as much as 15° owing in part to some angular divergence of the fluorescence light in our setup. In this case, the $\cos\Delta$ term in Eq. (1) does not vanish and the measured circular polarization P_3 will be influenced by P_1 (P_2 is practically zero, see Sec. III). To avoid erroneous P_3 measurements, the circular polarization P_3 was measured by choosing $\beta=0^\circ$ and by varying α since for $\beta=0^\circ$ the P_1 -dependent term containing $\cos\Delta$ vanishes.

III. EXPERIMENTAL RESULTS

We have first measured the total excitation cross section for Na $3s-3p$ excitation which to our knowledge is not reported in the literature. In order to avoid calibration problems associated with absolute measurements, we measured the excitation cross section for Ne^+ -ion impact relative to that for electron impact. The absolute cross section for electron impact at impact energies in the keV range is known within a few percent and allows a reliable normalization³² (typical cross section for 3-keV electron impact: $0.92 \times 10^{-16} \text{ cm}^2$). The absolute accuracy of our excitation cross sections for Ne^+ impact (Fig. 3) is ap-

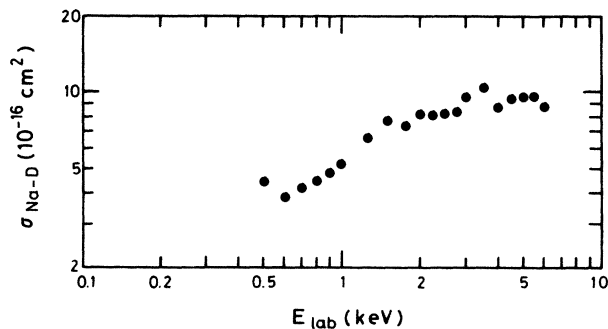


FIG. 3. Apparent excitation cross sections (including cascades) of the Na $3p$ state by Ne^+ ions vs impact energy. The absolute accuracy of the experimental data amounts to about 30%.

proximately 30%; the uncertainty is due to possible systematic errors as, e.g., incomplete charge collection by the Faraday cup, and a somewhat different overlap with the Na target for the primary beams of Ne^+ ions and electrons. The total cross sections were measured without polarization optics; accordingly the anisotropy of the radiation emission should be taken into account in the data evaluation. However, since the anisotropies (obtainable from the measured linear polarization P_1 of the Na D line) for Ne^+ ion and electron impact are equal within 2% in the investigated energy range (Fig. 4 of the present work and Fig. 3 of Ref. 33), a corresponding correction is superfluous.

The measured linear polarization P_1 (Fig. 4) depends only weakly on impact energy. P_1 reflects a collision-induced anisotropy of the excited $3p$ state. This anisotropy may be described by the alignment parameter \mathcal{A}_{20} which is related to the measured polarization P_1 (cf., e.g., Ref. 33):

$$\mathcal{A}_{20} = [2P_1 / (P_1 - 3)] / \bar{G}_2. \quad (2)$$

This formula holds if the electron spin is decoupled *during* the collision (see below), but is affected by fine and hyperfine coupling after the collision (Percival-Seaton hypothesis⁹). The factor \bar{G}_2 accounts for the depolarization by this coupling, for the $3p$ state of ^{23}Na : $\bar{G}_2 = 0.0982$.³³ The measured polarization (Fig. 4) amounts to $P_1 = -0.045$, and from Eq. (2) we get $\mathcal{A}_{20} \approx 0.30$. From

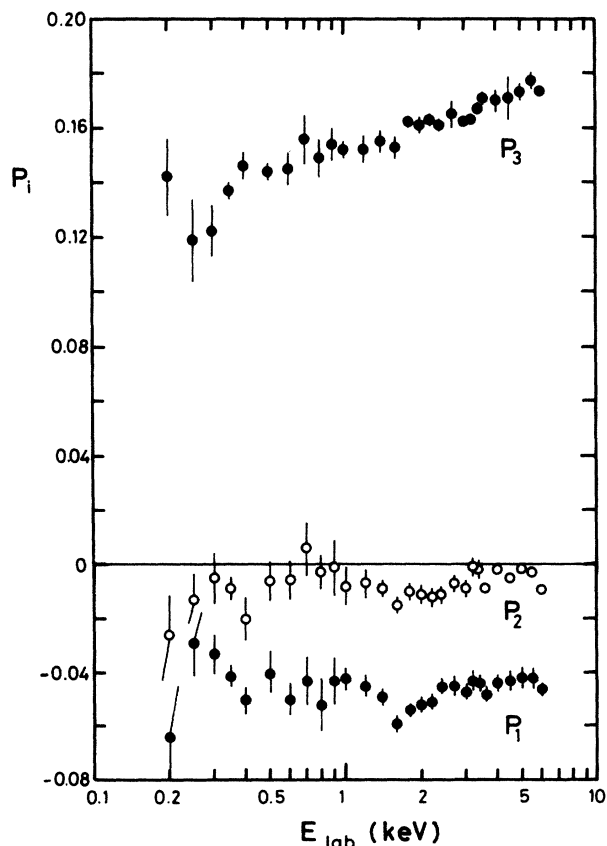


FIG. 4. Measured Stokes polarization parameters P_1 , P_2 , and P_3 of the unresolved Na $D_{1,2}$ line induced by Ne^+ impact. Errors given take only the statistical uncertainty into account.

this alignment value \mathcal{A}_{20} we can derive the relative excitation cross sections σ_1, σ_0 for the magnetic substates $|m_l| = 1, 0$ (the m_l quantum number is here related to a coordinate frame with the z axis parallel to the impact axis which differs from the coordinate frame of spin polarization). From the definition of the alignment \mathcal{A}_{20} of a p state (cf., e.g., Ref. 34),

$$\mathcal{A}_{20} = (\sigma_1 - \sigma_0) / (2\sigma_1 + \sigma_0), \quad (3)$$

and the experimental value $\mathcal{A}_{20} = 0.30$ we finally obtain

$$\sigma_1 \approx 3\sigma_0. \quad (4)$$

Therefore, in our collision process mainly $|m_l| = 1$ vacancies are produced.

The light polarization parameters P_2 and P_3 yield further information on the collisional interaction. For a non-coincident experiment with rotational symmetry around the impact axis these parameters vanish due to symmetry reasons. In our experiment, the rotational symmetry is broken by the transverse spin orientation of the Na atoms. Possible finite values of P_2 and P_3 then reveal specific spin effects during the collision.²² A P_2 value different from zero would indicate in the present case a noticeable interaction of the spin-orbit type between the spin of the target electron and the projectile orbit. Such an interaction might result from the combined action of two interactions listed in Table I. However, this combined action is not expected to be strong as is confirmed by the experimental data showing a linear polarization P_2 (Fig. 4) which is compatible with zero.

The circular polarization P_3 is a measure of the spin orientation of the excited $3p$ electron since spin-orbit coupling in the Na $3p$ state transfers an orientation of the spin to an orientation of the orbital angular momentum. The measured circular polarization P_3 (Fig. 4) has finite value, it changes its sign if the spin orientation of the Na beam is reversed. For our experimental geometry P_3 is related to the properties of the excited $3p$ state by the expression³³

$$P_3 = \frac{\sqrt{3} \langle T(I)_{10}^\dagger \rangle}{\sqrt{2} \langle T(I)_{00}^\dagger \rangle + \langle T(I)_{20}^\dagger \rangle}, \quad (5)$$

where $\langle T(I)_{kq}^\dagger \rangle$ denotes a state multipole characterizing the spatial charge cloud of the $3p$ ($l=1$) state. More precisely, the state multipoles in Eq. (5) are related to a coordinate frame with the z axis parallel to the axis of spin orientation and represent values averaged over the lifetime of the precessing excited state. $\langle T(I)_{10}^\dagger \rangle$ describes the orientation and $\langle T(I)_{20}^\dagger \rangle$ the alignment of the excited state.³⁵ Using the angular momentum algebra for fine and hyperfine coupling, the time-averaged state multipoles in Eq. (5) can be expressed in terms of the momentary state multipoles *immediately after* the collision.³³ The corresponding expressions are lengthy sums containing various nuclear state multipoles besides electronic state multipoles. In order to work out the basic ideas we neglect smaller terms [e.g., we put $\langle T(I)_{20}^\dagger \rangle = 0$] and thus we obtain the approximate relationship³³

$$P_3 \approx (0.572 + 0.265 P'_S / P_S) P_S, \quad (6)$$

where P_S is the initial spin polarization of the valence electron and the Na nucleus (which are identical for the applied technique of beam polarization by a hexapole magnet³³); P'_S denotes the final spin polarization of the valence electron immediately after the collision. For an estimated initial spin polarization $P_S = 0.205$ we obtain $P_3 = 0.172$ in case of spin conservation during the collision (i.e., $P'_S = P_S$), and $P_3 = 0.117$ in case of complete depolarization (i.e., $P'_S = 0$). Comparison of these predictions with the experimental data shows (Fig. 4) that at high impact energies the spin orientation is conserved within the experimental accuracy, but with decreasing impact energy there is a significant loss of spin orientation. We note that this interpretation of our polarization data is only applicable if the detected fluorescence light results from direct $3s$ - $3p$ excitation only and cascades from higher states feeding the $3p$ population can be neglected. This assumption will be justified below.

IV. DISCUSSION OF THE EXCITATION PROCESS

The excitation of Na($3p$) in collisions of the elements neon and sodium in the keV-energy regime has already been the subject of previous studies. For example, the system Ne + Na was studied in Refs. 10 and 36–39. The system Ne + Na⁺ was studied in Refs. 40 and 41. The Na $3p$ excitation cross sections reported for these systems are smaller than 0.6×10^{-16} cm² for impact energies E_{lab} below 6 keV. In contrast, our cross-section data for the Ne⁺ + Na system are much larger; they increase up to 10×10^{-16} cm² at the highest measured impact energy $E_{\text{lab}} = 6$ keV (Fig. 3). This result can easily be explained: In collisions of the two neutral atoms Ne + Na, no long-range Coulomb interaction is present, and excitation of Na $3p$ occurs only when the atoms almost “touch” each other; in collisions of Ne + Na⁺, the production of Na $3p$ requires the ionization of Ne, effective again at small internuclear distances. More precisely, for these two collision systems excitation occurs via electron promotion along the $4f\sigma$ molecular orbital at internuclear distances of about $1.6a_0$.⁴¹ In contrast, for the Ne⁺ + Na system studied in the present work the Na $3s$ - $3p$ excitation requires only 2.1 eV energy and may easily be induced by long-range Coulomb interaction with the Ne⁺ ion as will now be discussed in more detail.

Our experimental data have been obtained for impact energies from 0.2 to 6 keV which correspond to impact velocities of 0.03–0.2 times the classical orbiting velocity of the $3s$ electron. In this fairly adiabatic regime the excitation can be treated in the framework of the molecular orbital model. Due to the lack of a detailed correlation diagram for the NeNa⁺ quasimolecule, we adopt a semi-quantitative diagram⁴¹ (Fig. 5). The excitation process is discussed in a one-electron picture involving the initial Na $3s$ valence electron, since the two cores Ne⁺ $2p^5$ and Na⁺ $2p^6$ are not seriously perturbed in the collision (except for internuclear distances smaller than about $2a_0$). As a mechanism for the experimentally observed Na $3s$ - $3p$ excitation we suggest the following process (compare Fig. 5). On the incoming part of the projectile trajectory the electron originally at the Na⁺ core in the $3s$ state is

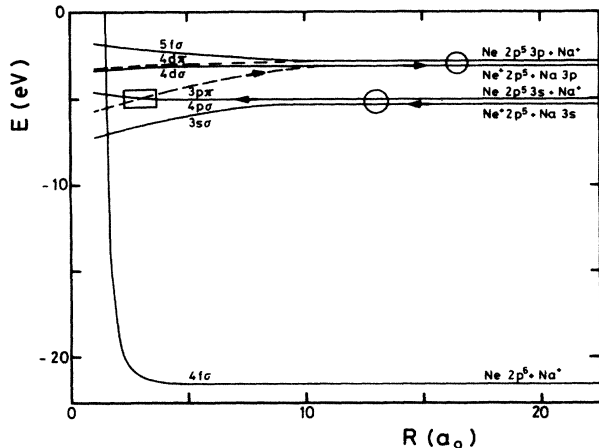


FIG. 5. Molecular orbital diagram of the NeNa^+ system (based on the diagrams of Ref. 41). On the right side the configurations for separated atoms are given. A circle (rectangle) denotes a radial (rotational) coupling.

transferred to the Ne^+ core into the $3s$ state ($\text{Ne } 2p^5 3s$ configuration). At smaller internuclear distances a $4p\sigma$ - $3p\pi$ rotational coupling occurs. On the outgoing part of the projectile trajectory the electron is distributed among the excited $3p$ states belonging either to the Na^+ or Ne^+ core. Finally, in the present experiment the $\text{Na } 3p$ population is detected by the emitted $\text{Na } D$ fluorescence light. According to the suggested excitation mechanism, we expect a comparable production of the $\text{Ne}(2p^5 3p)$ and the $\text{Na}(3p)$ excited states.^{40,41} The fluorescence of Ne , however, is harder to investigate experimentally, since strong fine-structure splitting of $\text{Ne}(2p^5 3p)$ and $\text{Ne}(2p^5 3s)$ distributes the total light intensity into a number of spectral lines which exhibit different polarization properties.

The experimentally observed preferential population of the $3p$ ($|m_l| = 1$) magnetic substate [Eq. (4)] is consistent with excitation via the $3p\pi$ state. The nonvanishing population of the $3p$ ($m_l = 0$) magnetic substate might be due to an incomplete adjustment of the electron wave function to the rotation of the internuclear axis, i.e., electron slipping. The measured excitation cross section varies between $(4-10) \times 10^{-16} \text{ cm}^2$ in the energy range studied (Fig. 3) which corresponds to the expected magnitude: The charge exchange at the incoming part of the trajectory is quite effective. The energy difference between the two channels $\text{Ne}^+(2p^5) + \text{Na}(3s)$ and $\text{Ne}(2p^5 3s) + \text{Na}^+$ is about 0.24 eV only (this value approximately holds for both fine-structure states of the $\text{Ne}^+ 2p^5$ core).⁴² According to model calculations⁴³ the cross section for this nearly resonant charge exchange amounts to approximately $10^{-15} - 10^{-14} \text{ cm}^2$ for impact energies from 0.2 to 6 keV. These cross sections are consistent with a radius of charge exchange of $R_0 = 13a_0$.⁴¹ Rotational coupling⁴⁴ occurs in the vicinity of the $4p\sigma$ - $3p\pi$ level crossing at internuclear distances of about $2a_0$ as inferred from the isoelectronic system NeNa^+ (Ref. 41) and Ne_2 (Ref. 45). On the outgoing part of the collision again almost-resonant electron transfer between the two channels $\text{Ne}(2p^5 3p) + \text{Na}^+$ and $\text{Ne}^+(2p^5) + \text{Na}(3p)$ occurs. The sharing ratio of direct to exchange $3p$ excitation is approximately 0.5 as can be es-

timated from the Demkov-Meyerhof formula^{46,47} and as has been confirmed experimentally.⁴⁰ Since the charge-exchange processes on the incoming and outgoing part of the trajectory occur with high probability at rather large internuclear distances, the $\text{Na } 3p$ excitation cross section is mainly determined by the $4p\sigma$ - $3p\pi$ rotational coupling. Our experimental data show that this coupling is strong for $\text{Ne}^+ + \text{Na}$, as is already known for the isoelectronic systems NeNa^+ from experiment⁴¹ and for Ne_2 from theory⁴⁵ which gives a value of 1.4 a.u. for the rotational matrix element.

Excitation of Na states higher than the $3p$ states is unlikely. For the collision velocities used in our experiment direct excitation by the Coulomb charge of the projectile is presumably negligible (compare measurements for various projectile ions⁴⁸). Molecular excitation via couplings with the promoted $4f\sigma$ state may occur; this requires small-distance collisions (below $1.6a_0$) resulting in cross sections smaller than $0.4 \times 10^{-16} \text{ cm}^2$ as follows from the experimental data for the $\text{Na}^+ + \text{Ne}$ system.^{49,41} Accordingly, cascade contributions to the observed $\text{Na } 3p$ population are expected to be small.

V. CHANGE OF SPIN ORIENTATION

The above discussion of the $3s$ - $3p$ excitation of Na in the $\text{Ne}^+ + \text{Na}$ collision system rests on a one-electron picture. In this framework the spin orientation of a single electron may be affected by the interaction of its orbital angular momentum l and its spin s . This spin-orbit interaction causes a splitting of energy levels by ΔE_{ls} and a precession of spin orientation in space with a period $\Delta t = h/\Delta E_{ls}$ (note h in the formula, not \hbar). For the $\text{Ne}^+ + \text{Na}$ system the spin-orbit interaction of the valence electron is weak: The interaction energy ΔE_{ls} for the quasimolecule is approximately equal to the energy for free atoms, since ΔE_{ls} depends only weakly on the internuclear distance.^{50,51} From spectroscopic data⁴² we get

$$\begin{aligned} \Delta t_{ls}(3s) &= \infty \quad \text{for Na } 3s, \\ \Delta t_{ls}(3s) &= \infty \quad \text{for Ne } 2p^5 3s, \\ \Delta t_{ls}(3p) &= c^{-1}/17 \text{ cm}^{-1} = 2 \times 10^{-12} \text{ s} \quad \text{for Na } 3p, \\ \Delta t_{ls}(3p) &= c^{-1}/5 \text{ cm}^{-1} = 1 \times 10^{-11} \text{ s} \quad \text{for Ne } 2p^5 3p. \end{aligned} \quad (7)$$

The spin precession times are thus much larger than the typical collision time $\Delta t = d/v$ where $d \approx 10a_0$ denotes interaction length and v the impact velocity:

$$\Delta t_{\text{coll}} = 6 \times 10^{-15} \text{ s} \quad (8)$$

for impact of 1-keV Ne ions. Accordingly, spin-orbit coupling of the valence electron during the collision is negligible in our experiment. An apparent change of spin orientation may result from the coupling dynamics of spin and orbital angular momentum at larger internuclear distances.^{15,17} Since this mechanism requires a nonvanishing orientation of the orbital angular momentum, it is not effective in the present noncoincident experiment.

The $\text{Ne}^+ + \text{Na}$ collision system is a one-hole-one-electron system and one expects similar effects as in one-electron-one-electron collision systems. Here the electron-electron interaction is a strong force yielding an interchange of electrons. In the interchange, the individu-

TABLE II. Splitting of Ne energy levels caused by the spin orbit and the exchange interaction expressed in terms of the interaction parameters ζ , G^0 , and G^1 (Ref. 52). The given values apply for the configurations $2p^5 3s$ and $2p^5 3p$ of the free Ne atom ("combined fit" of Ref. 54), compare also the recent parametrization in Refs. 55 and 56.

Level splitting	Ne $2p^5 3s$	Ne $2p^5 3p$
ΔE_{ls} ($2p^5$)	$\frac{3}{2}\zeta_{2p} = 777 \text{ cm}^{-1}$	$\frac{3}{2}\zeta_{2p} = 817 \text{ cm}^{-1}$
ΔE_{ls} ($3p$)		$\frac{3}{2}\zeta_{3p} = 5 \text{ cm}^{-1}$
ΔE_{xc} (triplet-singlet)	$\frac{2}{3}G^0(2p\ 3s) = 1487 \text{ cm}^{-1}$	$2G^0(2p\ 3p) = 1490 \text{ cm}^{-1}$

all electrons carry their spin orientation with them. Thus in collisions of a polarized atom with an unpolarized atom the spin orientation of the initially polarized atom may be strongly affected.^{20,21} The spin orientation oscillates in time with a characteristic frequency $\Delta E_{xc}/h$ where ΔE_{xc} is the splitting of energy levels caused by the exchange energy, i.e., the energy difference between triplet and singlet states. The final polarization P'_S of an electron with initial polarization P_S is given by²¹

$$P'_S = P_S \left[1 + \cos \left[\int dt \Delta E_{xc}/\hbar \right] \right] / 2$$

$$= P_S \left[1 + \cos \left[\int dR \Delta E_{xc}/v\hbar \right] \right] / 2, \quad (9)$$

where the integration extends over the projectile trajectory $R(t)$.

The collision process studied in the present work involves the Ne $2p^5 3s$ and Ne $2p^5 3p$ configurations as intermediate states. In these states strong exchange interaction between the $2p^5$ core and the $3s$ (or $3p$) valence electron as well as strong spin-orbit interaction in the $2p^5$ core is present. Since corresponding interaction energies for the molecular NeNa⁺ system are not available, we adopt the interaction energies for the free Na atom as a rough estimate (Table II). The exchange energy in both configurations of interest is almost the same $\Delta E_{xc} \approx 1490 \text{ cm}^{-1}$ which corresponds to an oscillation time $\Delta t = h/\Delta E$ for the spin orientation

$$\Delta t_{xc} = 3 \times 10^{-14} \text{ s}. \quad (10)$$

Thus, Δt_{xc} lies within a factor of 5 in the regime of the collision time Δt_{coll} [Eq. (8)]. Using Eq. (9) the final polarization can be calculated. We assume a straight-line projectile trajectory and treat the collision process with the following simplifying assumptions (compare Fig. 5).

On the incoming part of the trajectory charge transfer between the initial Na $3s$ state and the Ne $3s$ state ($2p^5 3s$ configuration) occurs at $R = 13a_0$.

Then the electron-exchange interaction becomes effective as determined by an exchange energy $\Delta E_{xc} = 0.5 \times 1487 \text{ cm}^{-1}$. By taking half of the exchange energy of the free Ne $2p^5 3s$ configuration (Table II) we account for sharing of the valence electron between the Na⁺ and Ne⁺ cores.

The distance of closest approach is $R \approx 3a_0$, corre-

sponding to the $4p\sigma$ - $3p\pi$ rotational coupling radius.

On the outgoing part of the trajectory, the electron-exchange interaction remains effective with an exchange energy $\Delta E_{xc} = 0.5 \times 1490 \text{ cm}^{-1}$, i.e., half of the value for the free Ne $2p^5 3p$ configuration (Table II), until the valence electron is finally transferred to the atomic Na $3p$ state at $R = 16.5a_0$.

All given distances have been taken from Ref. 41. Accordingly, electron exchange is effective over a region of $23.5a_0$ of the projectile trajectory with a strength of 745 cm^{-1} . Equation (9) allows us to calculate the final spin polarization P'_S and Eq. (6) to derive the expected circular light polarization P_3 (Fig. 6). As expected, spin change is small at high collision energies since for short times no significant electron exchange can take place. With decreasing impact energy, the interaction time increases and we observe an increasing spin depolarization. Quantitatively, our simple model with no free parameters somewhat overestimates the observed effect of depolarization; this defect may be easily removed by reducing the exchange energies or the length of the interaction region by

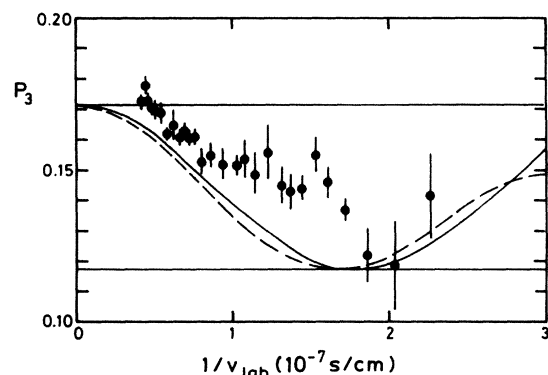


FIG. 6. Measured and calculated circular polarization P_3 of the fluorescence light vs inverse impact velocity v_{lab} . Upper and lower straight lines correspond to conservation of spin orientation ($P'_S = P_S$) and full depolarization ($P'_S = 0$), respectively, during the collision. The two other curves correspond to spin depolarization by electron exchange between the Ne⁺ $2p^5$ core and valence electron; spin-orbit coupling in Ne⁺ $2p^5$ neglected [—, Eq. (9)], and approximately taken into account [---, Eq. (11)].

a factor of about 1.5. Nevertheless the agreement is quite satisfactory regarding the crude treatment of the excitation process.

Finally, we estimate the influence of the spin-orbit interaction of the $\text{Ne}^+ 2p^5$ core (which has been neglected so far) on the spin depolarization of the valence electron. For this purpose, we approximate the actual intermediate coupling of the $\text{Ne } 2p^5 3s$ and $\text{Ne } 2p^5 3p$ configurations by LS coupling. Spin-orbit coupling of $3p$ in $\text{Ne } 2p^5 3p$ can be neglected as it is very weak. The spin depolarization can then be calculated in the formalism of coupling three angular momenta (see, e.g., Refs. 35 and 52). With the nomenclature l_2 and s_2 for orbital angular momentum and spin of the $2p^5$ configuration and s_1 for the spin of the $3s$ or $3p$ electron the LS -coupling results in the formation of $[(s_1 s_2)_S l_2]_J$ eigenstates, and the final spin polarization is given by

$$P_S' = \frac{P_S}{(2s_2 + 1)(2l_2 + 1)} \times \sum_{S', S, J', J} (2S' + 1)(2S + 1)(2J' + 1)(2J + 1) \times \begin{Bmatrix} S' & J' & l_2 \\ J & S & 1 \end{Bmatrix}^2 \begin{Bmatrix} s_1 & S' & s_2 \\ S & s_1 & 1 \end{Bmatrix}^2 \times \cos[(E_{S'J'} - E_{SJ})T/\hbar], \quad (11)$$

where $T = \int dt$ denotes the interaction time. As expected, Eq. (11) reduces to Eq. (9) for $l_2 = 0$, i.e., vanishing spin-orbit interaction in the $2p^5$ core. Using the interaction energies from Table II and making the same assumptions for the collision process as given above, the depolarization according to Eq. (11) has also been calculated (dashed curve in Fig. 6). As it turns out, the spin-orbit interaction in the $\text{Ne } 2p^5$ core has only little influence on the spin depolarization of the valence electron for $\text{Ne}^+ + \text{Na}$ collisions in the investigated energy range.

VI. CONCLUSIONS

Ion-atom collision systems involving a single active electron represent simple cases which are now well understood. Here the only spin-affecting mechanism is the

spin-orbit interaction causing a precession of spin orientation in space. Since the precession time is larger than the typical time of an energetic collision, the spin orientation is almost fixed during a region of small internuclear distances. Nevertheless, interesting spin effects may arise from the dynamics of transitions between molecular states [Hund's coupling case (a)] and atomic states [Hund's coupling case (c)]. These effects reveal details of the collision process at large internuclear distances, as shown by quantitative calculations (see, e.g., Ref. 17).

In collision systems with (at least) two active electrons, the electron exchange acts as another spin-affecting mechanism. Depending on the relative orientations of both spins, the collision system may be in a triplet state (both spins parallel) or in a superposition of singlet and triplet states (both spins antiparallel). According to Pauli's principle the symmetry properties of the total spatial wave function are determined by the spin state. The symmetry effects become large in the case of strong overlap of the individual wave functions. Thus, spin effects by the electron exchange probe the collisional interaction at small internuclear distances. The collision system $\text{Ne}^+ + \text{Na}$ studied in the present work shows a depolarization of spin orientation in the excitation process. This observation is the first experimental evidence of spin change caused by electron exchange in energetic atomic collisions. The observed depolarization yields information on the detailed interaction of a valence electron and a hole in an unfilled shell, i.e., on electron transfer during the collision. We are able to explain the experimental data semiquantitatively in spite of the complexity of the $\text{Ne}^+ + \text{Na}$ collision system. Decisive information on the fundamental exchange interaction is expected from simpler collision systems, e.g., $\text{He}^+ + \text{Na}$. Corresponding theoretical⁵³ and experimental work is in progress.

ACKNOWLEDGMENTS

Valuable discussions with Dr. H. Schmidt are gratefully acknowledged. The work has been supported by the Deutsche Forschungsgemeinschaft through Sonderforschungsbereich 216.

*Present address: Physikalisch-Technische Bundesanstalt, Institut Berlin, 1000 Berlin 10, Federal Republic of Germany.

†Present address: Department of Physics and Astronomy, Louisiana State University, Baton Rouge, Louisiana 70803.

‡Permanent address: Atomic Physics Laboratory, University of Stirling, Stirling FK9 4LA, Scotland.

¹N. Andersen and S. E. Nielsen, *Comments At. Mol. Phys.* **18**, 265 (1982).

²I. V. Hertel, H. Schmidt, A. Bähring, and E. Meyer, *Rep. Prog. Phys.* **48**, 375 (1985).

³U. Fano, *Rev. Mod. Phys.* **29**, 74 (1957).

⁴B. Bedersen, *Comments At. Mol. Phys.* **1**, 41 (1969); **2**, 7 (1970).

⁵M. Ya. Amusia, *Comments At. Mol. Phys.* **8**, 61 (1979).

⁶*Coherence and Correlation in Atomic Collisions*, edited by H.

Kleinpoppen and J. F. Williams (Plenum, New York, 1980).

⁷*Abstracts of the XIVth International Conference on the Physics of Electronic and Atomic Collisions, Palo Alto, 1985*, edited by M. J. Coggiola, D. L. Huestis, and R. P. Saxon (ICPEAC, Palo Alto, 1985).

⁸E. Wigner, *Nachr. Ges. Wiss. Göttingen* **374** (1927).

⁹I. C. Percival and M. J. Seaton, *Philos. Trans. R. Soc. London* **251**, 113 (1958).

¹⁰W. Mecklenbrauck, J. Schön, E. Speller, and V. Kempter, *J. Phys. B* **16**, 3271 (1977).

¹¹A. Bähring, E. Meyer, I. V. Hertel, H. Schmidt, *Z. Phys. A* **320**, 141 (1985).

¹²W. Jitschin, S. Osimitsch, H. Reihl, D. W. Mueller, H. Kleinpoppen, and H. O. Lutz, *Abstracts of the XIVth International Conference on the Physics of Electronic and Atomic Collisions*,

- Palo Alto, 1985*, edited by M. J. Coggiola, D. L. Huestis, and R. P. Saxon (ICPEAC, Palo Alto, 1985).
- ¹³K. Blum and H. Kleinpoppen, *Adv. At. Mol. Phys.* **19**, 187 (1983).
- ¹⁴G. F. Hanne, *Phys. Rep.* **95**, 95 (1983).
- ¹⁵F. van den Berg, P. Bijl, and R. Morgenstern, *Z. Phys. A* **320**, 1 (1985).
- ¹⁶E. E. Nikitin and S. Ya. Umanskii, *Theory of Slow Atomic Collisions* (Springer, Berlin, 1984), Chap. 11.
- ¹⁷H. Schmidt, A. Bähring, and R. Witte, *Z. Phys. D* **1**, 71 (1986).
- ¹⁸H. M. Gibbs and R. J. Hull, *Phys. Rev.* **153**, 132 (1967).
- ¹⁹D. Beck, U. Henkel, and A. Schultz, *Phys. Lett.* **27A**, 277 (1968).
- ²⁰D. R. Swenson, D. Tupa, and L. W. Anderson, *J. Phys. B* **18**, 4433 (1985).
- ²¹W. Jitschin, *Z. Phys. D* **1**, 135 (1986).
- ²²K. Bartschat and K. Blum, *Z. Phys. A* **304**, 85 (1982).
- ²³A. Wolcke, K. Bartschat, K. Blum, H. Borgmann, G. F. Hanne, and J. Kessler, *J. Phys. B* **16**, 639 (1983).
- ²⁴W. Jitschin, in *Fundamental Processes in Atomic Collision Physics*, edited by H. Kleinpoppen, J. S. Briggs, and H. O. Lutz (Plenum, New York, 1985), p. 539.
- ²⁵M. Lambropoulos and S. E. Moody, *Rev. Sci. Instrum.* **48**, 131 (1977).
- ²⁶D. Hils, W. Jitschin, and H. Kleinpoppen, *Appl. Phys.* **25**, 39 (1981).
- ²⁷R. Kollath, in *Landolt-Börnstein*, edited by J. Bartels *et al.* (Springer, Berlin, 1959), Vol. II/6, p. 1004.
- ²⁸N. L. S. Martin and A. von Engel, *J. Phys. D* **10**, 863 (1977).
- ²⁹C. E. Kuyatt, in *Methods of Experimental Physics*, edited by B. Bederson and W. L. Fite (Academic, New York, 1968), Vol. 7A, p. 1.
- ³⁰K. Bartschat, K. Blum, G. F. Hanne, and J. Kessler, *J. Phys. B* **14**, 3761 (1981).
- ³¹W. H. McMaster, *Am. J. Phys.* **22**, 351 (1954).
- ³²W. Jitschin, S. Osimitsch, D. W. Mueller, H. Reihl, R. J. Allan, O. Schöller, and H. O. Lutz, *J. Phys. B* **19**, 2299 (1986).
- ³³W. Jitschin, S. Osimitsch, H. Reihl, H. Kleinpoppen, and H. O. Lutz, *J. Phys. B* **17**, 1899 (1984).
- ³⁴E. G. Berezko and N. M. Kabachnik, *J. Phys. B* **10**, 2467 (1977).
- ³⁵K. Blum *Density Matrix Theory and Applications* (Plenum, New York, 1981).
- ³⁶J. Østgaard Olsen, N. Andersen, and T. Andersen, *J. Phys. B* **10**, 1723 (1977).
- ³⁷E. Horsdal Pedersen, P. Wahnon, C. Gaussorgues, N. Andersen, T. Andersen, K. Bahr, M. Barat, C. L. Cocke, J. Østgaard Olsen, J. Pommier, and V. Sidis, *J. Phys. B* **11**, L317 (1978).
- ³⁸N. Andersen, T. Andersen, K. Bahr, C.L. Cocke, E. Horsdal Pedersen, and J. Østgaard Olsen, *J. Phys. B* **12**, 2529 (1979).
- ³⁹C. Courbin-Gaussorgues, P. Wahnon, and M. Barat, *J. Phys. B* **12**, 3047 (1979).
- ⁴⁰N. H. Tolk, J. C. Tully, C. W. White, J. Kraus, A. A. Monge, D. L. Simms, M. F. Robbins, S. H. Neff, and W. Lichten, *Phys. Rev. A* **13**, 969 (1976).
- ⁴¹J. Østgaard Olsen, T. Andersen, M. Barat, Ch. Courbin-Gaussorgues, V. Sidis, J. Pommier, J. Agusti, N. Andersen, and A. Russek, *Phys. Rev. A* **19**, 1457 (1979).
- ⁴²C. E. Moore, *Atomic Energy Levels*, Natl. Bur. Stand. (U.S.) Circ. No. 467 (U.S. GPO, Washington, D.C., 1949), Vol. I.
- ⁴³D. Rapp and W. E. Francis, *J. Chem. Phys.* **37**, 2631 (1962).
- ⁴⁴A. Russek, *Phys. Rev. A* **4**, 1918 (1971).
- ⁴⁵J. P. Gauyacq, *J. Phys. B* **11**, 85 (1978).
- ⁴⁶Yu N. Demkov, *Zh. Eksp. Teor. Fiz.* **45**, 195 (1963) [*Sov. Phys.—JETP* **18**, 138 (1964)].
- ⁴⁷W. E. Meyerhof, *Phys. Rev. Lett.* **31**, 1341 (1973).
- ⁴⁸A. M. Howald, L. W. Anderson, and C. C. Lin, *Phys. Rev. Lett.* **51**, 2029 (1983).
- ⁴⁹V. P. Belik, S. V. Bobashev, and S. P. Dmitrier, *Zh. Eksp. Teor. Fiz.* **67**, 1674 (1974) [*Sov. Phys.—JETP* **40**, 833 (1975)].
- ⁵⁰H. Haberland, *Z. Phys. A* **307**, 35 (1982).
- ⁵¹G. Aepfelback, A. Nennemann, and D. Zimmermann, *Chem. Phys. Lett.* **96**, 311 (1983).
- ⁵²E. U. Condon and H. Odabasi, *Atomic Structure* (Cambridge University Press, Cambridge, England, 1980).
- ⁵³A. Riera (private communication).
- ⁵⁴R. Mehlhorn, *J. Opt. Soc. Am.* **59**, 1453 (1969).
- ⁵⁵W. Bussert, T. Bregel, J. Ganz, K. Harth, A. Siegel, M.-W. Ruf, H. Hotop, and H. Morgner, *J. Phys. (Paris) Colloq.* **46**, C1-199 (1985).
- ⁵⁶D. Hennecart and F. Masnou-Seeuws, *J. Phys. B* **18**, 657 (1985).